Journal of Earth Science, Vol. 23, No. 3, p. 285–296, June 2012 *ISSN 1674-487X*
Printed in China
DOI: 10.1007/s12583-012-0257-2

Analysis of Slope Stability with Dynamic Overloading from Earthquake

Ti Zhao (赵体), **Jinzhong Sun*** (孙进忠), **Bin Zhang** (张彬), **Cheng Li** (李程)
School of Engineering & Technology, *China University of Geosciences*, *Beijing* 100083, *China*

ABSTRACT: The analysis of slope earthquake stability is one of the most important research subjects in geotechnical engineering and earthquake engineering. Two different concepts of slope earthquake stability are put forward: strength reserve stability and dynamic overloading stability. The first concept of slope earthquake stability has been widely accepted, and relative analysis methods are also well developed; the second one, however, is seldom mentioned until now, and the failure criterion and the analysis method based on this concept are yet to be explored. What are researched are just the failure criterion and the analysis method of dynamic overloading earthquake stability. The criterion of critical earthquake peak acceleration for the dynamic overloading stability of a slope and its analysis method, the load increasing method (LIM), are put forward. The dynamic overloading earthquake stability of a loess slope at Changshougou (长寿沟) in Baoji (宝鸡) City, Shaanxi (陕西) Province, China, is analyzed with LIM. The analysis result reveals that the dynamic overloading earthquake stability of the slope is quite high to the action of the earthquake ground motion, with exceeding probability of 10% in the next 50 years.

KEY WORDS: slope, dynamic overloading, earthquake stability, load increasing method, critical earthquake peak acceleration.

INTRODUCTION

The analysis of slope earthquake stability is one of the most important research subjects in geotechnical engineering and earthquake engineering (Huang et al., 2010; Tang et al., 2010; Wei et al., 2010). Methods such as pseudo-static (e.g., Sun et al., 2008; Li, 2004) and finite element (e.g., Zheng et al., 2009; Dai and Li, 2007; Liu et al., 2003) are commonly used in the assessment of slope earthquake stability coefficient. Up to now, most mechanical analyses of slope earthquake stability mainly focus on the anti-sliding stability of slopes under a certain fortification earthquake action with a fixed intensity (e.g., Zheng et al., 2009; Li et al., 2007; Liu et al., 2005). In consideration of all situations of slope strength conditions and seismic loads, this paper argues that two different concepts of slope earthquake stability should be distinguished: strength reserve earthquake stability and dynamic overloading earthquake stability. The first concept means how much strength does the present slope reserves relative to its critical strength that is degenerated from its present strength until to the dynamic failure of the slope under the earthquake action of certain intensity. What is concerned in this kind of slope stability is the influence of the variation in

This study was supported by the National Natural Science Foundation of China (No. 40902086).

*Corresponding author: sjz@163.com

Manuscript received April 12, 2011.
Manuscript accepted July 2, 2011.

slope strength on slope earthquake stability. The meaning of the second concept is how strong a seismic load is needed to damage a slope in its present strength state dynamically, which can be evaluated by contrast between the critical earthquake action that just makes the slope damaged and the earthquake action as the local earthquake-resistant fortification standard. What is concerned in this kind of slope stability is the influence of the variation in earthquake intensity on slope earthquake stability. The similar concept has been set up to analyze the stability of a slope suffering a static overload (Wu et al., 2006). For these two different kinds of slope earthquake stability problems, the analyzing processes are somewhat different too. For the first, relative to a fixed seismic load intensity level, search for the critical strength state of the slope and define dynamic stability coefficient of the slope by the ratio of present strength to the critical strength of the slope. This is so-called strength reduction method (SRM) (Zheng et al., 2009). For the second, relative to the present strength state of a slope, search for the critical seismic load intensity that just makes the slope failure. Such a procedure can be named as load increasing method (LIM). Detailed comparison between SRM and LIM is listed in Table 1. The first concept of slope earthquake stability has been widely accepted, and relative analysis methods are also well developed; the second one, however, is seldom mentioned until now, and the failure criterion and the analysis method based on this concept are yet to be explored (Sun et al., 2010). According to the concept of dynamic overloading earthquake stability, LIM based on "critical earthquake peak acceleration searching" raised by Sun et al. (2010) is improved further and applied to the earthquake stability analysis of Changshougou slope in Baoji City, Shaanxi Province, China.

Table 1 Comparison between SRM and LIM

Category	Focus	Solving process	Definition of earthquake stability coefficient
SRM	Influence of variation in slope strength on slope earthquake stability	Reduce strength parameters c, φ gradually to search for the critical strength parameters c', φ'	$c'=c/F$, $\varphi'=\arctan(\tan(\varphi/F))$; c, φ: cohesion and internal frictional angle before reduction; c', φ': cohesion and internal frictional angle after reduction; F: reserved strength slope earthquake stability
LIM	Influence of variation in seismic intensity on slope earthquake stability	Increase seismic load intensity step by step to search for the critical seismic load	$K_d=a_c/a_m$; a_c: critical earthquake peak acceleration; a_m: local fortification peak acceleration; K_d: dynamic overloading earthquake stability

LIM FOR DYNAMIC OVERLOADING EARTHQUAKE STABILITY OF SLOPE

Every method for analysis of slope earthquake stability has its own physical consideration and suitable application scope. It is appropriate to use SRM to analyze slope failure, owing to strength reduction caused by weathering, water infiltration, and so on. However, what is mainly concerned in the problems of slope earthquake stability is how strong an earthquake should be to make a slope failure dynamically rather than self-degeneration of rock or soil strength of a slope. Therefore, dynamic LIM should be suitable for the analysis of slope earthquake stability. In addition, the earthquake damage of a slope is an indication of a break in the constitutive relationship of the rock or soil mass in the slope. During the analysis of slope earthquake stability with dynamic LIM, the action of earthquake force begins from a weak level and gradually increases to the critical intensity that just makes the slope reach the state of dynamic failure. Because the break in constitutive relationship of rock or soil mass in slope is avoided by searching the critical intensity of earthquake action from weak to strong, there should be no very large departure between the constitutive relationship used in the analysis and the actual situation of rock or soil mass in the slope. Concrete procedure of LIM is as follows.

(1) Select a suitable time process $a(t)$ of earthquake ground motion with a peak acceleration a_m according to the result of seismic risk analysis and the fortification level of the site where the slope is located.

(2) Get an approximate peak acceleration a_{pc} of critical earthquake action to the slope by pseudo-static method and adjust the amplitudes of the time process $a(t)$ to make the peak acceleration a_{p0}=a_{pc} then conduct test calculation with the earthquake action of the time process with adjusted amplitudes. If the calculation result shows that the slope is damaged by the earthquake action, zoom out the amplitude of the time process with a large multiple n and try the calculation again. Continue such kind of amplitude adjustment until the slope is not damaged anymore; the last time process $a_1(t)$ of earthquake ground motion will be the initial one for critical peak acceleration searching.

(3) Search for the time process of critical earthquake ground motion that just makes the slope failure occur by enlarging the amplitude of initial earthquake ground motion step by step with an increment $\beta a_1(t)$ (increment coefficient β<1, determined by calculating accuracy), and the critical peak acceleration a_c can be obtained from the time process of critical earthquake ground motion.

(4) Set up the failure criterion of the slope with critical earthquake peak acceleration a_c and fortification earthquake peak acceleration a_m as follows: define K_d=a_c/a_m as the coefficient of dynamic overloading earthquake stability of the slope; the slope is steady when K_d>1, the slope is in critical state when K_d=1, and the slope is unsteady when K_d<1.

The analysis procedure described above is shown in Fig. 1. The core of the procedure is searching for the peak acceleration of critical earthquake ground motion that just makes a slope damaged by increasing the intensity of earthquake ground motion gradually from weak to strong, so LIM can also be described as the method of critical earthquake peak acceleration searching. As far as we can see, there are at least five significant advantages that resulted from this new analysis approach. 1. Its physical meaning is clear and conforms to slope failure mechanism under earthquake action. 2. In consideration of the break in the constitutive relationship of the rock or soil mass in a slope before and after the slope is damaged by earthquake action, rational dynamic responses to different levels of earthquake intensities can be obtained by applying earthquake action that is gradually increased from a rather low intensity. 3. By setting up the earthquake stability criterion based on the critical earthquake peak acceleration a_c of a slope and the local fortification earthquake peak acceleration a_m of the district where the slope is located, the exceeding probability of a_m obtained from seismic risk analysis is introduced into the estimation of slope earthquake stability, which may greatly help us with understanding the failure probability of a slope under earthquake action. 4. Both the strength reserve of a slope relative to local fortification earthquake action and the critical earthquake intensity of the slope can be obtained from this analysis method. 5. The instantaneous kinetic energy of the sliding mass detached from a slope by

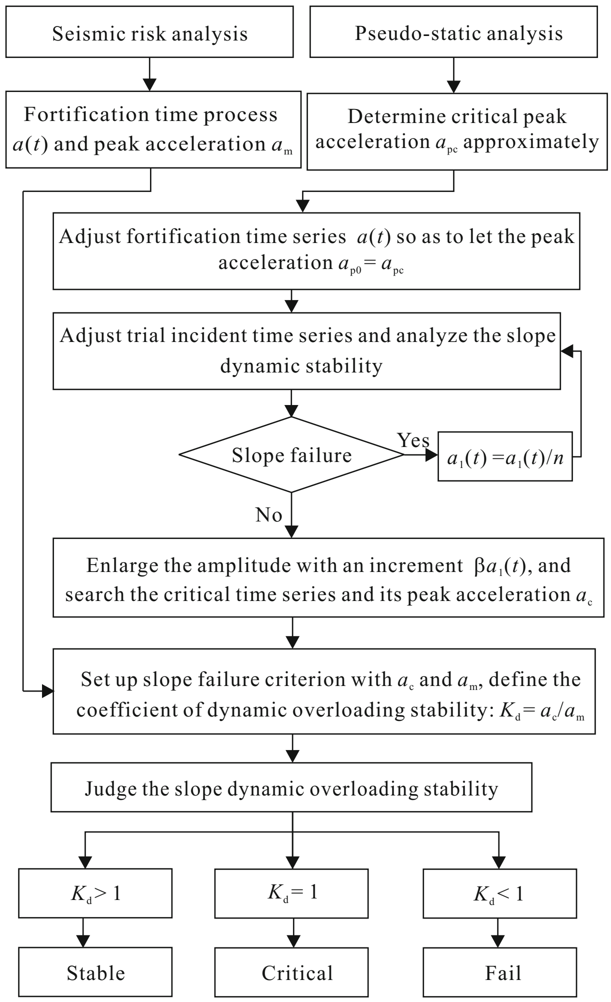

Figure 1. Flow chart of LIM.

earthquake action can be obtained at the moment when the slope failure occurs, which will offer an initial condition for kinematic study on earthquake landslide.

CASE STUDY

In order to demonstrate the application effect of LIM for slope earthquake stability, Changshougou slope in Baoji City was chosen as an analyzing example. A three-dimensional numerical model of the slope was set up according to the geotechnical condition of the slope, and the finite difference software FLAC^{3D} is adopted to simulate the dynamic response and failure pattern of the slope to the action of the earthquake ground motion with an appropriate seismic time series.

General Situation of the Slope

Changshougou loess slope is located at the fourth terrace on the north shore of Wei River, Jintai District, Baoji City. The whole terrace has a uniform deposit with dualistic structure and steady engineering geological properties, and the geological formation of the slope can be mainly divided into two layers: (1) top layer, Quaternary loess stratum (loess or silty clay), and (2) bottom layer, Pliocene strata, including red clay (*Hipparion* laterite) and valley interbedded sediments of mudstone and gravels (Sanmen series). Cut out by Changshougou, the slope has a general single slope surface dipping gently to the east. The digital elevation model (DEM) of the slope is shown in Fig. 2.

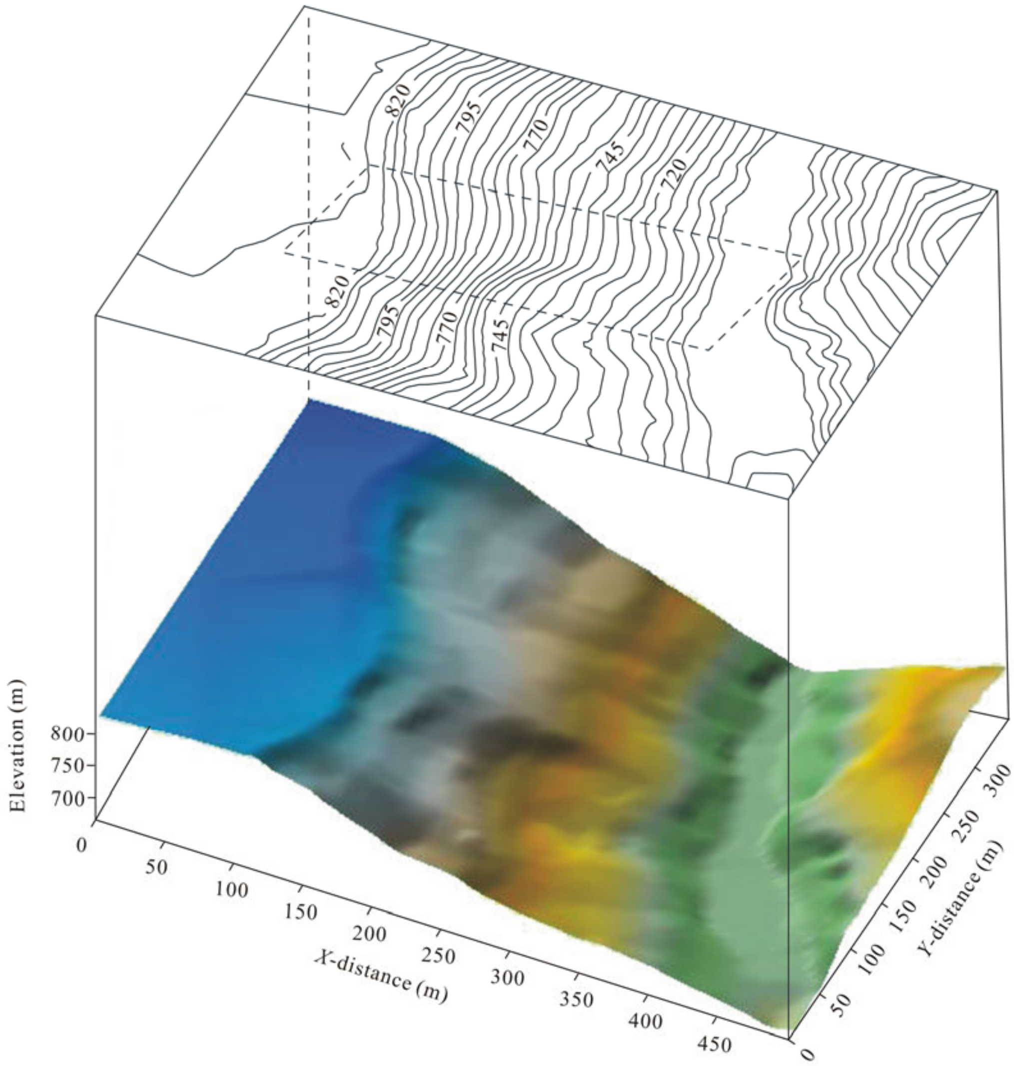

Figure 2. DEM model of Changshougou loess slope.

Analysis Model and Parameters of the Slope

Model coordinate system: set up the origin at the geographical point (107°06′10″E, 34°24′10″N) and have *X*-axis pointing to the east, *Y*-axis to the north, and *Z*-axis perpendicularly upward.

Model size: 310 m in direction *X* and 150 m in direction *Y*. The bottom boundary of the model is on the elevation 638 m.

Model materials: according to the drilling data of the slope site and the requirement of the numerical simulation, the rock and soil mass in the slope is divided into two layers (Fig. 3), and the relevant physical and mechanical parameters are listed in Table 2. Mohr-Coulomb plastic model built in the software FLAC^{3D} is applied as the constitutive relationship of the materials in the slope model, and local dumping with coefficient a_L=10% is set to the materials of the slope model. There is no pore water in the material of the model because the underground water table at the site of the slope is much lower than the bottom boundary of the slope model. Set gravity acceleration g=10.0 m·s^{-2}.

Model boundary conditions: quiet (viscous) boundary is set to the bottom, and free-field boundaries are utilized on four sides of the slope model.

Failure criterion: the critical failure state of the slope will be confirmed when plastic zones and the maximum shear strain increment transfix the slope body simultaneously (Zheng et al., 2009), and the critical peak acceleration will also be generated from the earthquake time series that is acting on the slope model at the same time.

Table 2 Physical and mechanical parameters of the Changshougou loess slope

Location	Superstrata	Substrata
Type of rock-soil	Quaternary loess	*Hipparion* laterite, Sanmen series
Bulk modulus K (MPa)	492.75	1 250.00
Shear modulus G (MPa)	267.72	860.66
Density ρ (kg/m^3)	1 800	2 066
Tensile strength τ (kPa)	12.0	240
Cohesion c (kPa)	55.5	690
Internal friction angle φ (°)	23.7	31.1

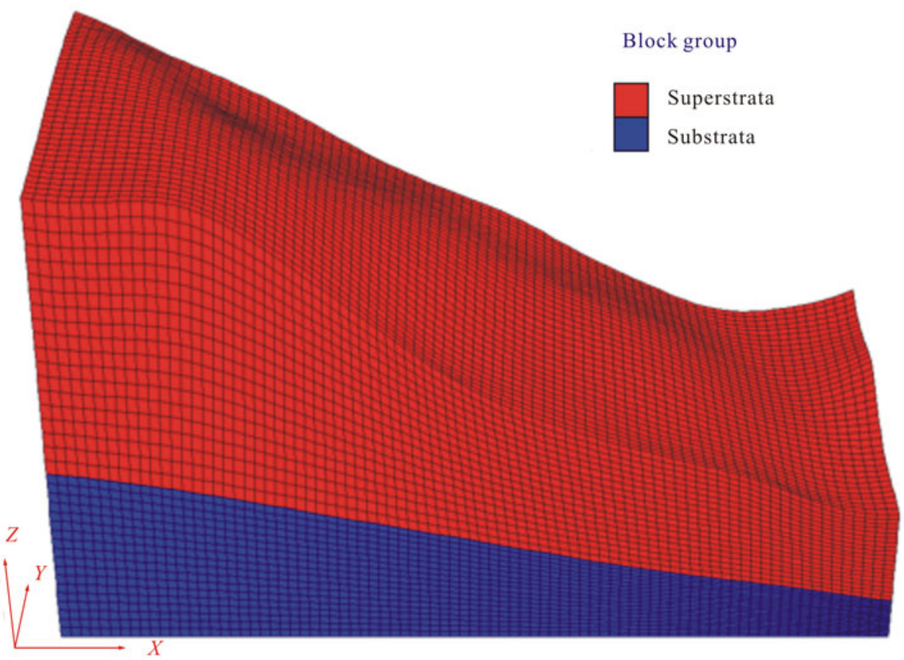

Figure 3. Numerical model of Changshougou loess slope.

Numerical Simulation of Slope Dynamic Overloading Stability

Synthesis of earthquake ground motion

It is always difficult to find a real seismic time series recorded with suitable conditions such as right epicentral distance and local site conditions that can meet up the requirements of seismic design. Thus, synthesizing an artificial time history of earthquake ground motion is a significant work in the anti-seismic analysis. The main methods for synthesis of earthquake ground motion are proportion method, target response spectrum fitting method, and empirical-theoretical method (Jiang and Dai, 1993). In this article, the time series of local fortification earthquake ground motion is created by target response spectrum fitting method as shown in formulas (1)–(8) (Zhao and Zhang, 2006; Hu and He, 1986; Cornell, 1968).

$$a(t)=f(t)\cdot x(t) \tag{1}$$

where $a(t)$—generated acceleration time history of earthquake ground motion, $f(t)$—intensity envelope function, and $x(t)$—stationary random vibration function. To obtain $f(t)$ and $x(t)$, combine (2) and (3)

$$f(t)=\begin{cases} (t/t_1)^{\lambda_1} & 0 \le t < t_1 \\ 1 & t_1 \le t < t_2 \\ e^{-\lambda_2(t-t_2)} & t_2 \le t < T \end{cases} \tag{2}$$

where t—duration of earthquake ground motion, T—total ground motion duration, t_1—starting time of the strong section of earthquake ground motion, t_2—finishing time of the strong section of earthquake ground motion, λ_1—shape parameter of envelope function prior to the strong section of earthquake ground motion, and λ_2—shape parameter of envelope function after the strong section of earthquake ground motion. λ_1 and λ_2 may be determined by intensity increasing section before strong sections of recorded earthquake ground motion and intensity decreasing section after strong section of recorded earthquake ground motion.

$$x(t)=\sum_{k=0}^{n-1} A(\omega_k)\cos[\omega_k t+\phi(\omega_k)] \tag{3}$$

where $\omega_k=k\Delta\omega$—circular frequency of the k^{th}-order vibration component, with $\Delta\omega=2\pi/T$; $\phi(\omega_k)$—random phase angle uniformly distributed in [0, 2π]; and $A(\omega_k)$—amplitude of the k^{th}-order vibration component, obtained from formula (4).

$$A(\omega_k)=2\sqrt{G(\omega_k)\cdot\frac{2\pi}{T}} \tag{4}$$

where $G(\omega)$—power spectrum transformed from $S_a^{\mathrm{T}}(\omega, \zeta)$ (target earthquake acceleration response spectrum). The relation between $G(\omega)$ and $S_a^{\mathrm{T}}(\omega, \zeta)$ can be summarized in formula (5) (Hu and He, 1986).

$$G(\omega)=\frac{\zeta}{\pi\omega}\cdot\frac{[S_a^{\mathrm{T}}(\omega,\zeta)]^2}{\ln\left[\dfrac{-\pi\ln(1-P)}{\omega T}\right]} \tag{5}$$

where ζ—damping ratio of target earthquake ground motion response spectrum and P—exceeding probability of target earthquake ground motion response spectrum.

Calculate the response spectrum $S_a(\omega, \zeta)$ of $a(t)$ from formula (1) and compare it with the target spectrum $S_a^{\mathrm{T}}(\omega, \zeta)$. There usually have some differences between $S_a(\omega, \zeta)$ and $S_a^{\mathrm{T}}(\omega, \zeta)$. In order to improve the conformity between the time histories of synthesis earthquake ground motion and of the target one, amplitude spectrum $A(\omega)$ should be adjusted in the light of formula (6) (fit $S_a(\omega, \zeta)$ to $S_a^{\mathrm{T}}(\omega, \zeta)$, i.e., spectrum fitting).

$$A^{i+1}(\omega_k)=\frac{S_a^{\mathrm{T}}(\omega_j,\zeta)}{S_a(\omega_j,\zeta)}A^i(\omega_k), \quad n_{1j}<k\le n_{2j},\ j=1, 2, \ldots, N \tag{6}$$

where $A^i(\omega_k)$ and $A^{i+1}(\omega_k)$—amplitudes of the i^{th} and $(i+1)^{\text{th}}$ iterative results, respectively; $S_a(\omega_j, \zeta)$ and $S_a^{\mathrm{T}}(\omega_j, \zeta)$—calculated spectrum and target spectrum at frequency-control point ω_j; and N—number of frequency-control points for spectrum fitting. The adjustment of $A(\omega)$ is confined in a number n_{2j}–n_{1j} of Fourier components adjacent to ω_j. Relative to n_{1j} and n_{2j}, ω_{1j}, and ω_{2j} are determined by formula (7)

$$\omega_{1j}=\frac{\omega_{j-1}+\omega_j}{2},\quad \omega_{2j}=\frac{\omega_j+\omega_{j+1}}{2},$$
$$n_{1j}=\frac{\omega_{1j}}{\Delta\omega},\quad n_{2j}=\frac{\omega_{2j}}{\Delta\omega} \tag{7}$$

where $(\omega_{1j}, \omega_{2j}]$ is called the master frequency-control band of ω_j, and to the control point ω_j, the iterative operation is only applied to the amplitudes within this frequency band. There are two reasons for confining the amplitude adjustment within the master frequency-control band: (1) in the light of resonance principle, only the frequency components in a narrow band around the frequency ω_j have evident effect on the amplitude $A(\omega_j)$, and (2) adjustment to $A(\omega_j)$ should not cause the variation of amplitudes on frequency points other than ω_j. After several times of iterative rectifications, the generated spectrum will reach a high similarity to the target spectrum. When the error between the two spectra matches the relationship given in formula (8), the spectrum fitting can be completed.

$$\delta = \frac{1}{N}\sum_{j=1}^{N}\frac{S_a(\omega_j,\zeta)-S_a^T(\omega_j,\zeta)}{S_a^T(\omega_j,\zeta)} < \varepsilon \tag{8}$$

where δ—relative difference between synthesized spectrum and target spectrum and ε—required precision (arbitrarily small).

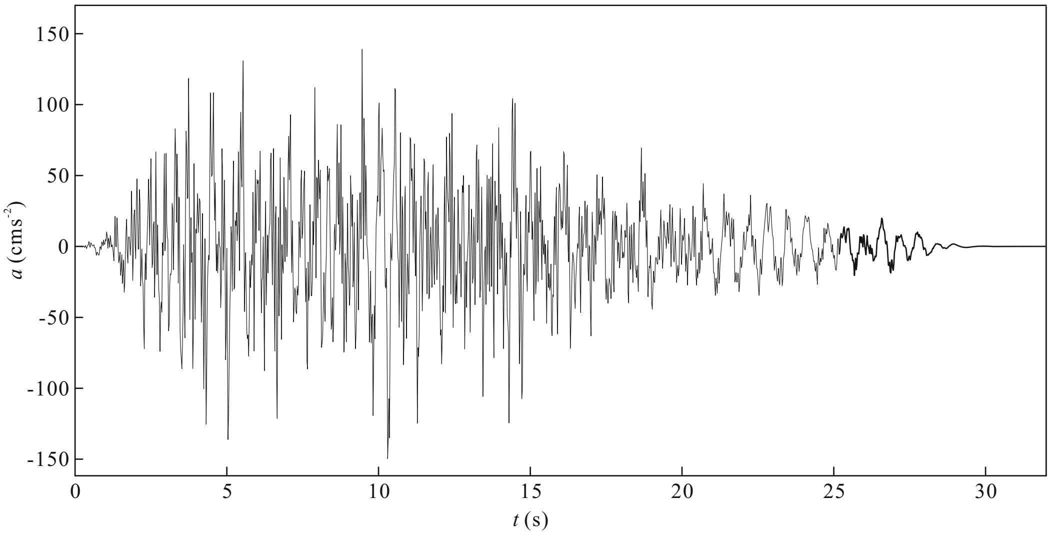

Figure 4. Time series of synthetic earthquake ground motion.

According to the national standard of the People's Republic of China, "Criterion of Architecture Aseismatic Design" (GB 50011-2010), the peak acceleration (a_m) of fundamental seismic design in Baoji City is 0.15 g and the basic seismic intensity is VII degree. To regulate the synthetic spectrum, the earthquake ground motion with 10% exceeding probability in the next 50 years is selected and used as the target spectrum. With 1 600 frequency-control points and 5% relative error, the fitted acceleration time history of earthquake ground motion satisfying the earthquake fortification target in Baoji City is shown in Fig. 4, and after suitable amplitude adjustment according to the procedure of LIM, the fitted acceleration time history will be used as the earthquake ground motion excitation in the analysis of slope earthquake stability.

Numerical analysis of slope earthquake stability

There are two steps in numerical analysis of slope earthquake stability: (a) set up the initial geostatic stress state of the slope and (b) perform the dynamic analysis.

Installation of initial geostatic stress state To obtain the proper initial geostatic stress state of the slope, static calculation is required before the dynamic analysis. Two procedures are followed in the static calculation: (a) set relevant mechanical parameters and take elastic model as material constitutive model and then make the slope model balanced in gravity field and (b) take Mohr-Coulomb model as the material constitutive model and then rebalance the model. The contour plot of vertical geostatic stresses in the slope in gravity field is shown in Fig. 5. This is just the slope model on which the increasing earthquake load will be applied.

Dynamic analysis Roughly determine the critical peak acceleration a_{pc} of the slope by pseudo-static analysis and adjust the amplitudes of the artificial acceleration time series $a(t)$ as shown in Fig. 4 according to the procedure of LIM. In this article, the initial ground motion peak acceleration (a_{p0}) is 200 cm·s^{-2}, with increment coefficient β=0.1.

Have seismic S-waves vertical shoot onto the bottom boundary of the slope, and set the particle vibration of S-waves parallel to the slope gradient direction (X-axis) in horizontal plane. Because of the static viscous boundary, earthquake load should be acted in the form of shear stress onto the bottom boundary of the slope, therefore, the acceleration time series $a(t)$ must be converted to stress time series $\tau_S(t)$ by formula (9)

$$\tau_S(t) = -2\rho C_S v_S(t) \tag{9}$$

where ρ—mass density, C_S—propagation velocity of S-wave, and $v_S(t)$—particle vibration velocity time history integrated from acceleration time series $a(t)$.

Simulated results Following the principle of LIM, gradually increase the intensity of earthquake action to search for the critical failure state of the slope. Simulated results are shown in Figs. 6–9.

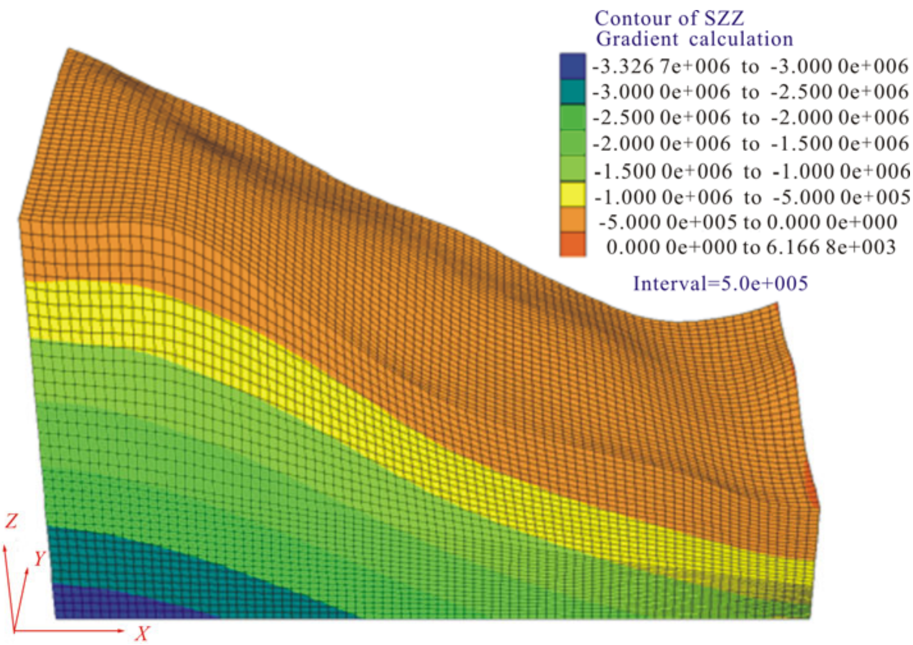

Figure 5. Contour plot of initial vertical geostatic stresses in the slope (unit: Pa).

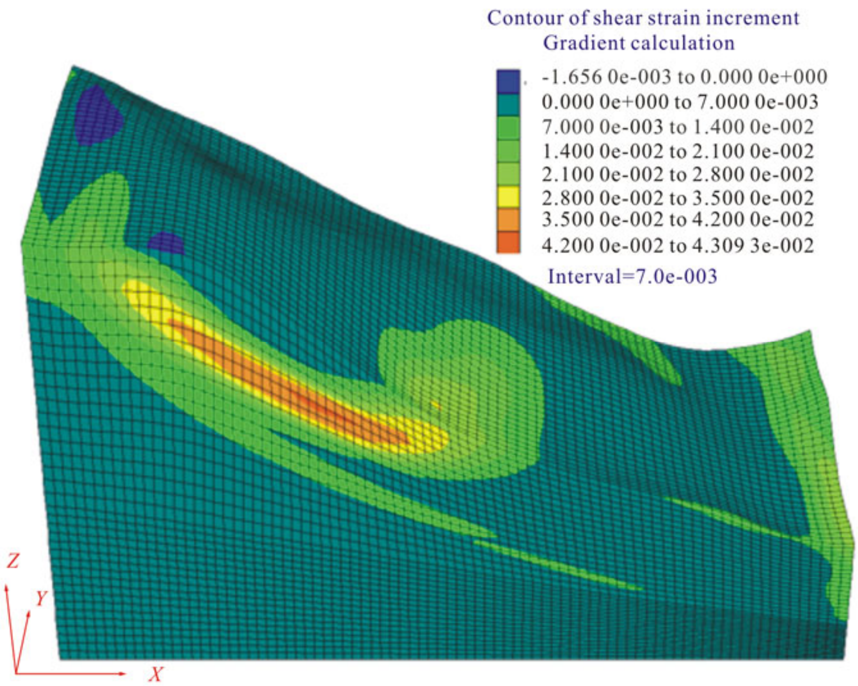

Figure 6. Contour of shear strain increment (unit: 1) of Changshougou loess slope caused by earthquake ground motion with peak acceleration a_p=220 cm·s^{-2}.

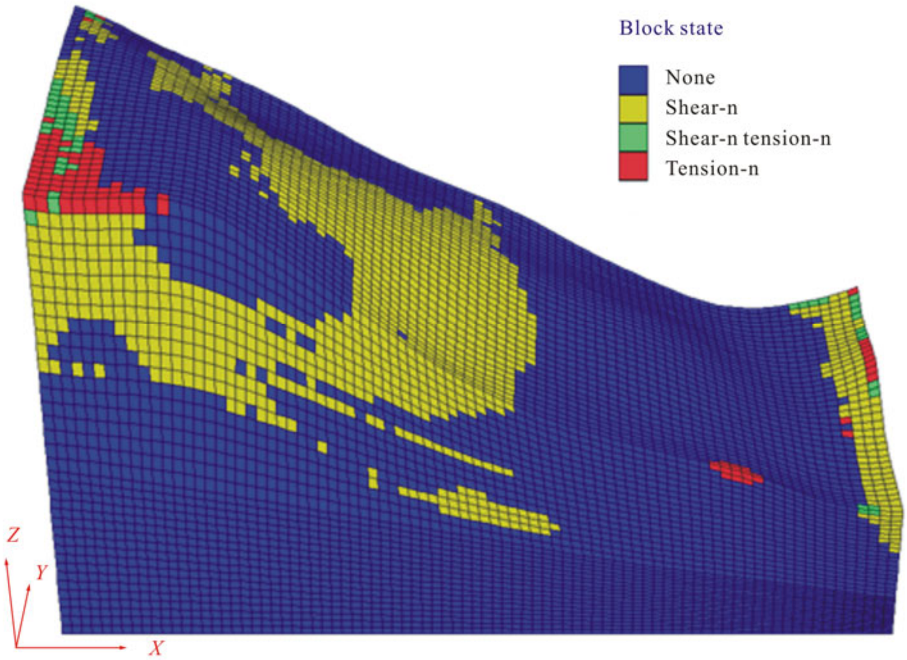

Figure 7. Plastic zones of Changshougou loess slope caused by earthquake ground motion with peak acceleration a_p=220 cm·s^{-2}.

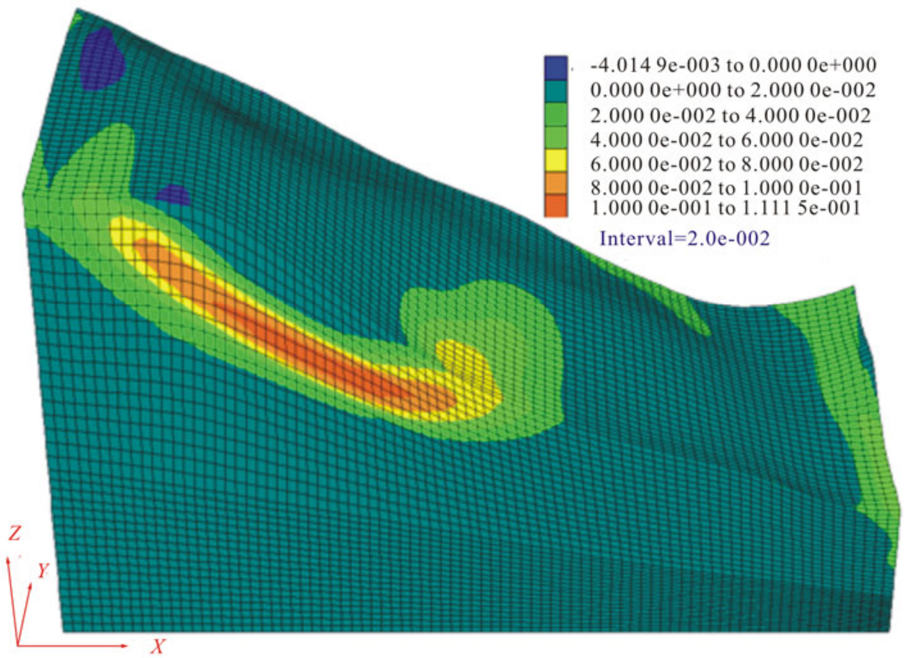

Figure 8. Contour of shear strain increment (unit: 1) of Changshougou loess slope caused by earthquake ground motion with peak acceleration a_p=300 cm·s^{-2}.

From Figs. 6 and 7, we can realize that when input earthquake peak acceleration (a_p) increases to 220 cm·s^{-2}, the relative maximum shear strain increment reaches up to 4.41%, and the slope begins to form a steady potential sliding belt; however, the tensile failure zones have not transfixed at the top of slope, which indicates that the slope is still in a steady state. Therefore, the intensity of earthquake action can be further increased.

With further increase of the intensity of earthquake action, failure phenomena of the slope are getting more and more evident. It is clearly displayed in Figs. 8 and 9 that with the intensity of earthquake action with peak acceleration a_p=300 cm·s^{-2}, the maximum shear strain increment is 11.1%, and the tensile fractures on the top of the slope have connected with potential sliding belt, which is formed with a transfixed plastic zones beneath the projecting portion on the upper slope (Fig. 9). By these phenomena, we can confirm that the slope has reached its critical failure state; thus, the critical earthquake peak acceleration value of the slope may be determined as a_c=300 cm·s^{-2}=0.30 g.

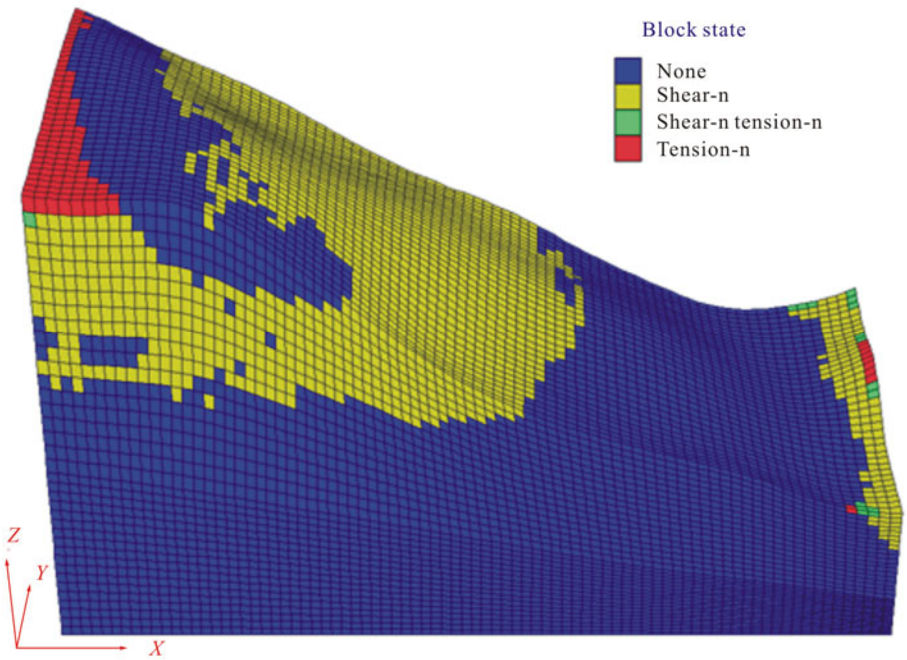

Figure 9. Plastic zones of Changshougou loess slope caused by earthquake ground motion with peak acceleration a_p=300 cm·s^{-2}.

Earthquake Stability of Changshougou Loess Slope

By the numerical simulation result of the dynamic overloading earthquake stability of Changshougou loess slope with LIM, the critical earthquake peak acceleration, a_c=300 cm·s^{-2}=0.30 g, of the slope is obtained; on the other hand, the fortification earthquake peak acceleration has been determined as a_m=150 cm·s^{-2}=0.15 g as shown in Fig. 4.

Based on the concept of dynamic overloading earthquake stability, the coefficient K_d of earthquake stability of Changshougou slope is determined as follows.

K_d=a_c/a_m=0.30 g/0.15 g=2.0

Now, we can see that Changshougou slope possesses high earthquake stability to the peak acceleration a_m=0.15 g of fortification earthquake ground motion with 10% exceeding probability in the next 50 years, and we can also find out that the exceeding probability of the peak acceleration a_m, in practice, has been introduced into the coefficient K_d of dynamic overloading earthquake stability of the slope.

CONCLUSIONS AND PERSPECTIVE

Based on the new concepts of slope seismic stability put forward in this paper, a new analysis method of the slope earthquake stability is developed, and the following results have been achieved.

(1) Two different concepts of slope earthquake stability are distinguished: 1) strength reserve earthquake stability that is displayed with the difference between the present strength of a slope and its critical strength to an earthquake action of certain intensity

and 2) dynamic overloading earthquake stability revealed by comparison between the critical earthquake action of the slope at its present strength and the fortification earthquake action as the local earthquake resistant target.

(2) In consideration of the fact that there is a break in the constitutive relationship of the rock or soil mass in a slope before and after the earthquake failure of the slope occurs, an idea of searching for the critical earthquake action of the slope at its present strength state by inputting the earthquake action from weak to strong is put forward, and a new optimized approach combining the pseudo-static method and the LIM to analyze dynamic overloading slope earthquake stability is formed.

(3) In light of the concept of dynamic overloading method, the criterion of earthquake stability is constructed. By this way, the traditional analysis method considering the comparison between inner stress and the strength of the slope is transformed to the method presented here, which mainly focuses on the comparison between the critical earthquake peak acceleration a_c and local fortification earthquake peak acceleration a_m. Thus, not only set up the connection between the slope earthquake stability and the possible earthquake action onto the slope in future but also transmit the exceeding probability of fortification peak earthquake acceleration to the coefficient of slope earthquake stability, which constitutes an important portion of the possibility of dynamic overloading slope earthquake stability.

(4) The analysis of dynamic overloading earthquake stability of Changshougou loess slope proves that the LIM based on searching for critical earthquake peak acceleration of a slope is a rational approach, which can provide us a better understanding of slope earthquake stability.

It should be noted that one time of dynamic overloading simulation of a slope can only reflect one type of dynamic slope failure of this slope. There should be multiple types of dynamic slope failures of the same slope due to the diversity of earthquake action. The diversity in dynamic slope failures of a slope induced by the variation of earthquake action should be studied further to lay a foundation for the analysis of earthquake slope failure probability. Furthermore, the analytical method of earthquake slope failure possibility in consideration of exceeding probability of fortification earthquake peak acceleration and the diversity of earthquake slope failures also needs to be further threshed.

This work extends the concept of earthquake slope stability and provides a new approach for its analysis. Particularly, the critical earthquake peak acceleration criterion to the failure of a slope at its present strength state forms a connection between the analysis of earthquake slope stability and the seismic risk analysis of the slope site and lays a foundation for further assessing earthquake slope failure probability. Such thought and its analysis approach can also be put forward into analyzing slope failures caused by other kinds of inducing factors such as wind erosion or rainfalls, so that a uniform risk estimation system for slope geological disasters can be prospected in the coming future.

REFERENCES CITED

Cornell, C. A., 1968. Engineering Seismic Risk Analysis. *Bulletin of the Seismological Society of America*, 58(5): 1583–1606

Dai, M. L., Li, T. C., 2007. Analysis of Dynamic Stability Safety Evaluation for Complex Rock Slopes by Strength Reduction Numerical Method. *Chinese Journal of Rock Mechanics and Engineering*, 26(Suppl. 1): 2749–2754 (in Chinese with English Abstract)

Hu, Y. X., He, X., 1986. Phase Angle Consideration in Generating Response Spectrum-Compatible Group Motion. *Earthquake Engineering and Engineering Vibration*, 6(2): 37–51 (in Chinese with English Abstract)

Huang, R. Q., Liu, W. H., Zhou, J. P., et al., 2010. Experimental Field Study of Movement Characteristics of Rock Blocks Falling down a Slope. *Journal of Earth Science*, 21(3): 330–339, doi:10.1007/s12583-010-0096-y

Jiang, P., Dai, L. S., 1993. Introduction to Engineering Seismology. Seismological Press, Beijing. 84–102 (in Chinese)

Li, H. B., Xiao, K. Q., Liu, Y. Q., 2007. Factor of Safety Analysis of Bedding Rock Slope under Seismic Load. *Chinese Journal of Rock Mechanics and Engineering*, 26(12): 2385–2394 (in Chinese with English Abstract)

Li, Z. S., 2004. Landslide Stability Analysis under Seismic Ground Motion. *Hydrogeology & Engineering Geology*, 2:

4–8 (in Chinese with English Abstract)

Liu, H. L., Fei, K., Gao, Y. F., 2003. Time History Analysis Method of Slope Seismic Stability. *Rock and Soil Mechanics*, 24(4): 553–557 (in Chinese with English Abstract)

Liu, J. L., Luan, M. T., Zhao, S. F., et al., 2005. Discussion on Criteria for Evaluating Stability of Slope in Elastoplastic FEM Based on Shear Strength Reduction Technique. *Rock and Soil Mechanics*, 26(8): 1345–1348 (in Chinese with English Abstract)

Sun, J. Z., Liu, Y. Q., Zhao, T., et al., 2010. Critical Acceleration Analysis of Slope Earthquake Stability. In: Williams, A. L., Pinches, G. M., Chin, C. Y., et al., eds., Proceedings of the 11th IAEG Congress. Auckland, New Zealand. 3641–3649

Sun, J. Z., Tian, X. F., Guan, X. D., et al., 2008. Stability Analysis for Loosened Rock Slope of Jinyang Grand Buddha in Taiyuan, China. *Earth Science Frontiers*, 15(4): 227–238 (in Chinese with English Abstract)

Tang, H. M., Jia, H. B., Hu, X. L., et al., 2010. Characteristics of Landslides Induced by the Great Wenchuan Earthquake. *Journal of Earth Science*, 21(1): 104–113, doi:10.1007/s12583-010-0008-1

Wei, F. Q., Chernomorets, S., Aristov, K., et al., 2010. A Seismically Triggered Landslide in the Niujuan Valley near the Epicenter of the 2008 Wenchuan Earthquake. *Journal of Earth Science*, 21(6): 901–909, doi:10.1007/s12583-010-0143-8

Wu, S. G., Zhang, Y. X., Kang, M., 2006. Application of Surcharge Method in Analysis of Rock Slope Stability. Proceedings of the Second National Academic Conference of Geotechnical Engineering (Volume One), Wuhan. 84–90 (in Chinese)

Zhao, F. X., Zhang, Y. S., 2006. Artificial Ground Motion Compatible with Specified Peak Velocity and Target Spectrum. *Acta Seismologica Sinica*, 28(4): 429–437 (in Chinese with English Abstract)

Zheng, Y. R., Ye, H. L., Huang, R. Q., 2009. Analysis and Discussion of Failure Mechanism and Fracture Surface of Slope under Earthquake. *Chinese Journal of Rock Mechanics and Engineering*, 28(8): 1714–1723 (in Chinese with English Abstract)